Available online at www.derpharmachemica.com

ISSN 0975-413X
CODEN (USA): PCHHAX

Der Pharma Chemica, 2017, 9(23):38-45
(http://www.derpharmachemica.com/archive.html)

Synthesis, Structural Elucidation of Aminoacetylenicoxyquinazoline and their Antiproliferative Activities

Zuhair A Muhi-eldeen[1*], Bara Alani[1], Elham N Al-Kaissi[2], Sanaa K Bardaweel[3], Mohammed Gattas[4], Tawfeeq Arafat[1]

[1]Department of Medicinal Chemistry and Pharmacognosy, Faculty of Pharmacy, University of Petra, Amman, Jordan, P.O. Box-961343 Amman, Jordan
[2]Department of Pharmaceutics and Pharmaceutical Technology, Faculty of Pharmacy, University of Petra, Amman, Jordan
[3]Department of Pharmaceutical Sciences, Faculty of Pharmacy, The University of Jordan, Amman-11942, Jordan
[4]College of Pharmacy, Al-Ain University of Science and Technology, Al-Ain, United Arab Emirates, Jordan

ABSTRACT

The aminoacetylenicoxyquinazoline were synthesized and their structures were confirmed through Infra-Red (IR), Proton Nuclear Magnetic Resonance (^{1}H-NMR), Carbon-13 Nuclear Magnetic Resonance (^{13}C-NMR) and elemental analysis. Docking with Epidural Growth Factor Receptor (EGFR) kinase were carried out and showed effective overlap. The aminoacetylenicoxyquinazoline were tested for their antitumor activities using breast (MCF) and colon (CaCO-2) cancer cell lines. All synthesized compounds exhibited antiproliferative activity but it was weaker than the well-known standard Doxorubicin. Further structural modifications are needed to enhance their antiproliferative effects.

Keywords: Aminoacetylenic, Quinazoline derivatives, Alkylation, Molecular modelling

INTRODUCTION

Kinase inhibitors of the epidermal growth factor receptor

An important focus of medicinal chemistry is to synthesis and study compounds with antiproliferative activities. One of the transmembrane receptor tyrosine kinase of the ErbB family that is abnormally activated in many epithelial tumors is the Epidermal Growth Factor Receptor (EGFR). This family is comprised of four related receptors which are the EGFR itself (EGFR/ErbB1/HER1), Receptor Tyrosine-Protein Kinase (ErbB2) (HER2/neu), ErbB3 (HER3), ErbB4 (HER4). These receptors trigger downstream signaling pathways that are not linear but consist of rich multilayered and cross-connected networks, allowing for horizontal interactions and permit multiple combinatorial responses. This may explain the variety of biological outcomes to activation of a specific receptor in a specific cell. Receptor activation leads to recruitment and phosphorylation of several intracellular substrates, which in turn engage mitogenic signaling and other tumor promoting activities. Deregulation of these tightly regulated ErbB receptor signaling pathways contributes to malignant transformation. Several mechanisms can lead to aberrant receptor activation, including receptor overexpression, activating mutations, overexpression of receptor ligands, gene amplification, and/or loss of negative regulatory mechanisms. The cell surface is where the initial ligand-receptor interaction occurs. ErbB receptors are composed of an extracellular ligand-binding region, a transmembrane segment, and an intracellular protein kinase domain with a regulatory carboxyl terminal segment. Several agents have been studied as kinase inhibitors [1-4] and first of these to reach the clinic was gefitinib oral, low-molecular-weight, Adenosine Triphosphate (ATP) competitive inhibitors of the receptor's tyrosine kinase (Iressa; Figure 1) [5-8].

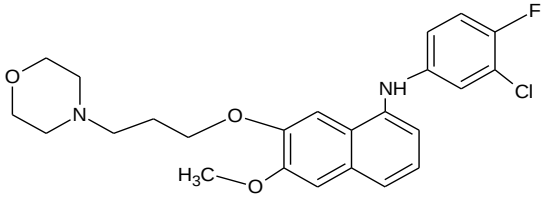

Figure 1: N-(3-chloro-4-fluorophenyl)-7-methoxy-6-(3-morphin-4-ylpropoxy)quinazolin-4-amine

Interviewing various structural features of different compounds which are in use or under investigation, such as gefitinib, erlotinib, lapatinib as EGFR inhibitors, we investigate a new and novel series of aminoacetylenic oxyquinozoline as EGFR for the following reasons: 4-hydroxyquiiinazoline as a fractional base analogue to quinazoline found in many EGFR inhibitors, aminoacetylenic moiety were represent the appropriate functional groups required to ensure interaction with EGFR as the basic amino group is required for ionic bonding with the corresponding groups on EGFR to induce the inhibitory activity and the 2-butyne group to provide the essential distance between the nitrogen of cyclic amine and oxyquinazoline; the aromatic ring which initiate π-overlap with the aromatic amino acid in the EGFR; the hydrocarbons in cyclic amine provide lipophilic interaction with the receptors as seen with ether derivative in many inhibitors; the oxygen ether to provide hydrogen bonding. Furthermore, the triple bond generates electrostatic interaction with corresponding EGFR. The preliminary *in vitro* clinical testing supports our rationalization in designing these compounds.

MATERIALS AND METHODS

Chemicals

The following chemicals were used: 4-hydroxyquinazoline 98% (Sigma Aldrich, USA), propargyl bromide (Sigma Aldrich, USA), piperidine 99% reagent plus (Sigma Aldrich, USA), 2-methylpiperidine 98% (Sigma Aldrich, USA), cis 2,6-dimethylpiperidine 98% (Sigma Aldrich, USA), pyrrolidine 98% (Sigma Aldrich, USA), N-methylpiperazine 99%, hexamethyleneimine 99% (Azepane), acetonitrile solvent HPLC (Sigma Aldrich, USA), Potassium carbonate (Gainland Chemical Company, UK), 1,4-dioxane (Full Time, China), paraformaldehyde (BDH chemicals Ltd Poole, England), ethanol (Gianland chemical company), cuprous chloride LRG (East Anglia Chemicals, Hadleighlpswich), Dimethyl Sulfoxide (DMSO) (BBC Chemicals for lab, EU).

Instrumentation

The structures of the synthesized compounds were confirmed by Infra-Red (IR), Proton Nuclear Magnetic Resonance (^{1}H-NMR), Carbon-13 Nuclear Magnetic Resonance (^{13}C-NMR), Differential Scanning Calorimetry (DSC) and elemental analysis. Melting points were determined on Gallenkamp Melting point Apparatus (California, USA). Infrared (IR) spectra were recorded on Bruker Fourier Transform Infra-Red (FTIR) spectrophotometer (Massachusetts, USA), using KBr discs and values were represented in cm^{-1}. ^{1}H-NMR and ^{13}C-NMR spectra were measured on a Varian 300 MHz spectrometer (Illinois, USA) and DMSO-d_6 as solvent with Tetramethylsilane (TMS) as the internal standard. ^{1}H data are reported in order: multiplicity (br, broad; s, singlet; d, doublet; t, triplet, m, multiplet). The elemental analysis was performed for C, H, N using (Euro EA elemental analyzer, Milan, Italy). The results obtained had a maximum deviation of ± 0.4 from the theoretical value, which is considered within the acceptable variation range in results (± 4. 4%). This variation range is set according to the accuracy of Euro EA Elemental Analyzer device, faculty of Pharmacy in the University of Jordan. DSC thermogram measurement was carried out by using the DSC 1 Stare System v.11. ox (Mettler Toledo, Zürich, Switzerland). Molecular docking was carried using PyMo1.9 Electrostatic interaction. ChemBioDraw (Massachusetts, U.S.A) was used in the drawing of our schemes.

Docking study

The EFGR-kinase domain used in this docking study was downloaded from the protein data bank (PDB: 1XKK) [9] then the co-crystallized ligand and all water molecules were removed from the protein structure. Protein atoms were given partial charges using Kollman united atom model in the Autodock Tool program [10,11]. The ATP binding site of the EFGR kinase domain was identified by its own co-crystallized ligand (lapatinib) then a grid box of a 60 × 50 × 60 Å size was created using the Autogrid module [12,13] with a grid spacing of 0.375 Å.

Ligand 3D structures were built then were energy minimized using the Maestro program [14] and the OPLS force field [15], respectively. Atomic partial charges were given for all ligands by Gasteiger-Marsili model [16] (tertiary amine groups were assigned as protonated). Next, ligands were docked into the ATP binding site using the Autodock software (version 4.2) [12,13] where the Lamarckian Genetic Algorithm [12] was employed for the conformational sampling process. Subsequently, docked poses were scored via the Autodock scoring function which includes terms for van der Waals, hydrogen bond, electrostatic interactions, and the ligand internal energy.

Biological study

MCF-7 and Caco-II cells were cultivated in Dulbecco's Eagle Modified Medium (DMEM, Biochrom, Berlin, Germany). All cell lines were cultured at 37°C and all media were supplemented with 1% of 2 mM L-glutamine (Lonza), 10% fatal calf serum (Gibco, Paisley, UK), 50 IU/ml penicillin/streptomycin (Sigma, St. Louis, MO) and amphotericin B (Sigma, St. Louis, MO). Cells from passage number 9-15 were used. For the cytotoxicity test, the examined compounds were added to the culture medium and incubated for 48 h incubation period in an atmosphere of 5% CO_2 and 95 relative humidity at 37°C.

Briefly, cells were seeded at a density of 8×10^3 cells per well in 96-well microplate in appropriate medium. At the end of the exposure period, 4,5-Dimethylthiazol-2-yl)-2,5-Diphenyl Tetrazolium Bromide (MTT) (Dorset, UK) assay was carried out as previously described (ISO, 2009). The yellow tetrazolium dye of MTT was reduced by metabolically active cells into an intracellular purple formation product. The absorbance values of each well were determined with a microplate Enzyme-linked Immune Sorbent Assay (ELISA) reader equipped with a 570 nm filter. Survival rates of the controls were set to represent 100% viability. Untreated cultures were used as control groups.

Synthesis

Synthesis of 4-(prop-2-yn-1-yloxy)quinazoline (alkylation reaction): A mixture of 4-hydroxyquinazoline (0.73 g, 0.005 mol), potassium carbonate K_2CO_3 (2.00 g), in 20 ml acetonitrile added to it mixture of propargyl bromide and 10 ml acetonitrile then refluxed up to 80°C and stirred for 75 min, after cooling, the insoluble residue was removed by filtration to give solution without color. The filtrate was concentrated under reduced pressure yielding the desired white solid compound (Scheme 1 and Figure 2). The instrumental and analytical data were as followed.

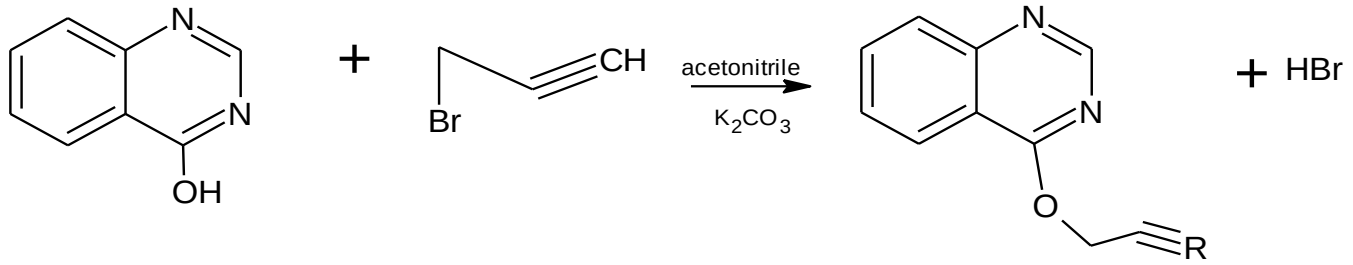

Scheme 1: Synthesis of 4-(prop-2-yn-1-yloxy) quinazoline

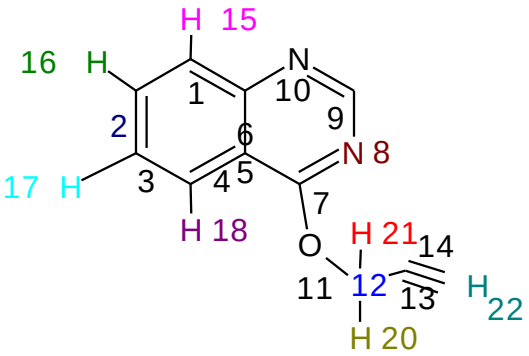

Figure 2: 4-(Prop-2-yn-1-yloxy)quinazoline

IR spectra (KBr cm^{-1}): 3300 (acetylenic C-H stretch), 3000 (acetylenic C-H stretch), 2100 (C≡C stretch), 1680 (Ar C=H stretch), 780 (Ar C-H stretch), ^{1}H-NMR (DMSO-d_6): δ (ppm): 3.09 (s, H22), 4.81 (s, H21), 7.68 (t, Ar, H17), 8.42 (s, H19). Elemental analysis: for $C_{11}H_8N_2O$: Calcd: C, 78.57%; H, 4.76%; N, 16.67%. Found: C, 78.66%; H, 4.77%; N, 16.88%.

Synthesis of 4-{[4-(amino-1-yl)but-2-yn-1-yl]oxy}quinazoline (BZ 1-6), (Mannich reaction): A mixture of 4-(prop-2yn-1-yloxy)quinazoline (0.92 g, 0.005 mol), paraformaldehyde (0.15 g, 0.005 mol) and cyclic amine around (0.005 mol), catalytic amount of cuprous chloride (0.03), in peroxide-free dioxin 35 ml was refluxed for 1 h. the solvent was removed under reduced pressure yielding green to blue semi solid residue for compounds BZ 1-6 (Figures 3 and 4). The IR spectra of 4-{[4-(amino-1-yl)but-2-yn-1-yl]oxy}quinazoline (BZ 1-6) showed the disappearance of terminal acetylenic proton at 3300 cm^{-1}, which indicate synthesis of compounds (BZ 1-6) and were consistent with the assigned structures. The instrumental and analytical data are presented in the results.

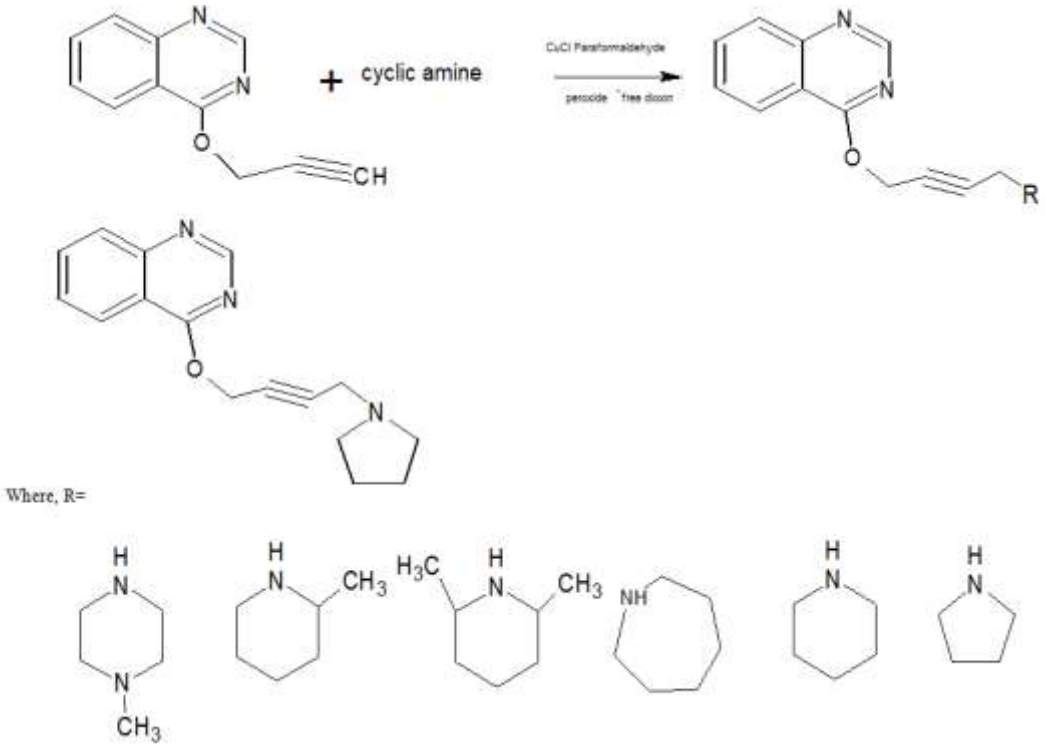

Scheme 2: Synthesis of 4-{[4-(amino-1-yl)but-2-yn-1-yl]oxy}quinazoline (BZ 1-6)

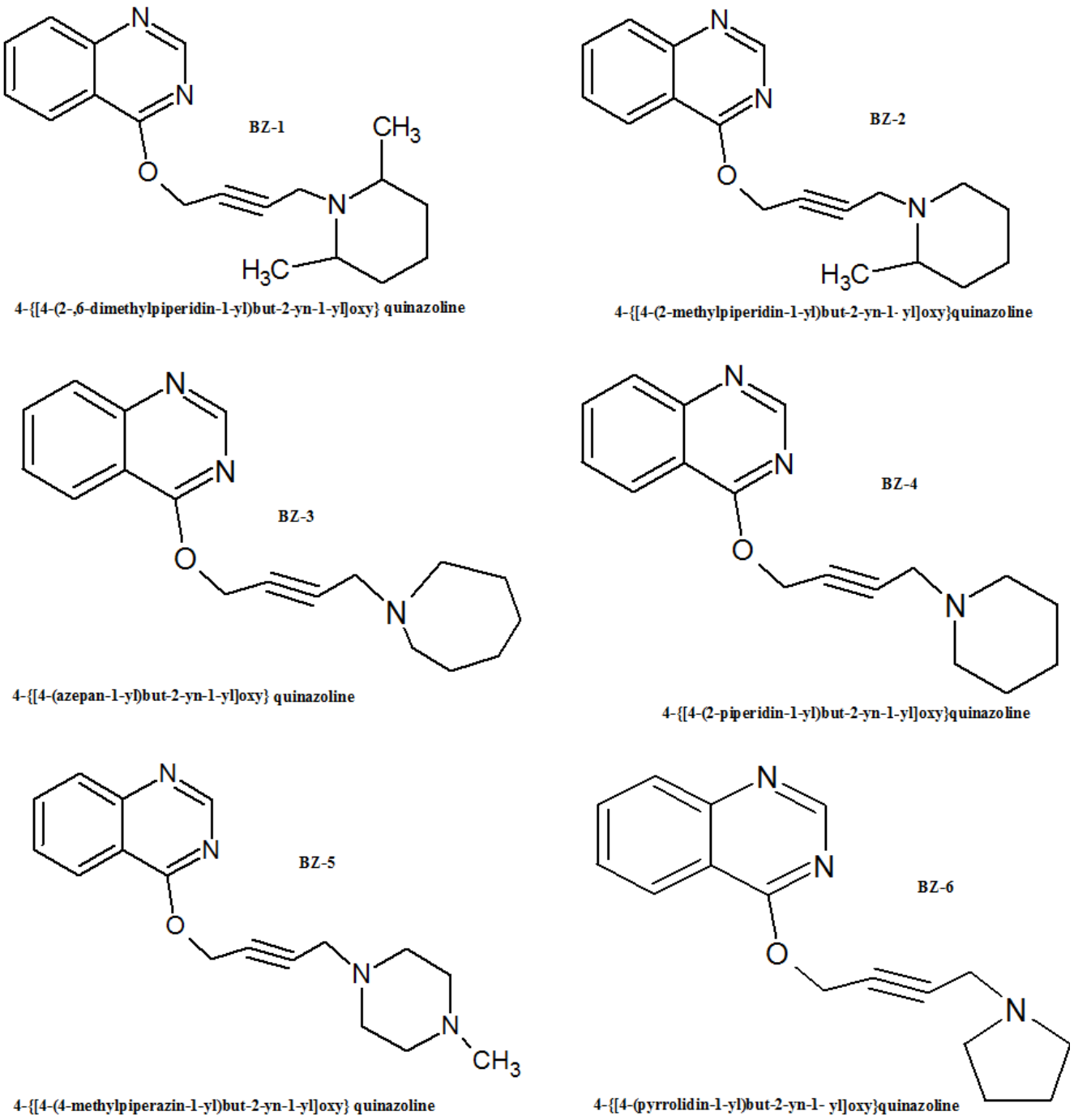

Figure 3: Compounds 4-{[4-(amino-1-yl)but-2-yn-1-yl]oxy}quinazoline (BZ 1-6)

The instrumental and analytical data of each compound were:

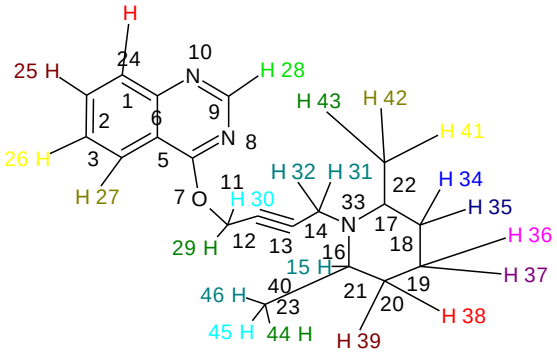

Figure 4: 4-{[4-(2-,6-dimethylpiperidin-1-yl)but-2-yn-1-yl]oxy}quinazoline

4-{[4-(2-,6-dimethylpiperidin-1-yl)but-2-yn-1-yl]oxy}quinazoline (BZ-1): IR spectra (KBr cm^{-1}): 2851 (C-H stretch), 1600 (Ar, C=C stretch), 1465 (C-C stretch), 1250 (C-O stretch), 1200 (C-N stretch), 870 (Ar, C-H bend), ^{1}H-NMR (DMSO-d_6): δ(ppm): 0.96 (m, various protons of cyclic amine, H34, 38), 1.10 (m, various protons of cyclic amine, H35, 39), 2.29 (m, various protons of cyclic amine, H33, 40), 3.31 (s, H31), 3.55 (s, H32), 4.86 (s, H29), 7.54 (t, Ar, H26), 8.47 (s, Ar, H28); ^{13}C-NMR (DMSO-d_6): δ(ppm): 21 (22, 23), 24 (19), 35 (18, 20), 37 (15), 54 (17, 21), 66 (12), 79 (13, 14), 126 (5), 127 (1, 3), 134 (2), 147 (9), 148 (6), 159 (7). Elemental analysis: for $C_{19}H_{23}N_3O$: Calcd: C, 78.57%; H, 4.76%; N, 16.67%. Found: C, 78.66%; H, 4.67%; N, 16.87%. MW 309.

4-{[4-(2-methylpiperidin-1-yl)but-2-yn-1- yl]oxy}quinazoline (BZ-2): IR spectra (KBr cm^{-1}): 2851 (C-H stretch), 1600 (Ar, C=C stretch), 1117 (C-O stretch), 1082 (C-N stretch), 870 (Ar, C-H bend). ^{1}H-NMR (DMSO-d_6), δ(ppm): 1.23 (m, various protons of cyclic amine, H36, H38), 1.53 (m, various protons of cyclic amine, H37, H39), 2.21 (t, H32), 2.64 (t, H33), 3.65 (s, H31), 4.86 (s, H29), 7.58 (t, Ar, H25), 8.48 (d, Ar, H26); ^{13}C-NMR (DMSO-d_6): δ(ppm): 19 (22), 24 (19), 26 (18), 34 (20), 43 (15), 53 (17), 54 (21), 80 (13), 85 (14), 126 (5), 127 (1, 3), 134 (2), 147 (9), 148 (6), 159 (7). Elemental analysis: for $C_{18}H_{21}N_3O$: Calcd: C, 78.57%; H, 4.76%; N, 16.67%. Found: C, 78.66%; H, 4.76%; N, 16.87%.

4-{[4-(azepan-1-yl)but-2-yn-1-yl]oxy}quinazoline (BZ-3): IR spectra (KBr cm^{-1}): 2921 (C-H stretch), 1600 (Ar, C=C stretch), 1472 (C-C stretch), 1320 (amine, C-N stretch), 1000 (C-O stretch), 770 (Ar, C-H bend); ^{1}H-NMR (DMSO-d_6), δ(ppm): 1.39 (m, various protons of cyclic amine, H36, H37), 1.67 (m, various protons of cyclic amine, H34, H35), 2.58 (t, various protons of cyclic amine, H32, H33), 3.44 (s, H30), 4.84 (s, H28), 7.54 (d, Ar, H23), 8.18 (d, Ar, H26). Elemental analysis: for $C_{18}H_{21}N_3O$: Calcd: C, 77.42%; H, 7.52%; N, 15.05%. Found: C, 77.22%; H, 7.44%; N, 15.32%.

4-{[4-(2-piperidin-1-yl)but-2-yn-1-yl]oxy}quinazoline (BZ-4): IR spectra (KBr cm^{-1}): 2850 (C-H stretch), 1690 (C=C stretch), 1253 (C-N stretch), 1116 (C-O stretch), 1082 (C-C, stretch), 870 (Ar, C-H bend). ^{1}H-NMR (DMSO-d_6): δ (ppm): 1.39 (m, various protons of cyclic amine, H35, H36), 1.45 (m, various protons of cyclic amine, H33, H34), 3.71 (s, H29), 4.77 (s, H27), 7.57 (t, Ar, H24), 7.71 (t, Ar, H23), 8.19 (d, Ar, H25); ^{13}C-NMR (DMSO-d_6): δ (ppm): 24 (19), 25(18, 20), 47 (15), 52 (17, 21), 53 (12), 79 (13), 81 (14), 126 (5), 127 (1, 3), 134 (2), 147 (9), 148 (6), 159 (7). Elemental analysis: for $C_{22}H_{19}N_3O$: Calcd: C, 78.57%; H, 4.76%; N, 16.66%. Found: C, 78.66%; H, 4.77%; N, 16.87%.

4-{[4-(4-methylpiperazin-1-yl)but-2-yn-1-yl]oxy}quinazoline (BZ-5): IR spectra (KBr cm^{-1}): 2792 (C-H stretch), 1681 (C=C stretch), 1456 (C-N stretch), 1365 (amine, C-N stretch), 1280 (C-C stretch), 1160 (C-O stretch), 1050 (amine, C-N stretch), 770 (Ar, C-H bend), 690 (Ar, C-H bend). ^{1}H-NMR (DMSO-d_6), δ(ppm): 2.28 (t, various protons of cyclic amine, H33, H39), 3.09 (t, various protons of cyclic amine, H38, H32), 3.41 (s, H29), 4.8 (s, H27), 7.55 (t, Ar, H24), 8.19 (t, Ar, H25); ^{13}C-NMR (DMSO-d_6), δ (ppm): 46 (22), 51 (17, 21), 55 (18. 20), 56 (12), 79 (13), 80 (14), 126 (5), 127 (1, 3), 134 (2), 147 (9), 148 (6), 159 (7). Elemental analysis: for $C_{17}H_{20}N_3O$: Calcd: C, 78.57%; H, 4.76%; N, 16.66%. Found: C, 78.66%; H, 4.77%; N, 16.87%.

4-{[4-(pyrrolidin-1-yl)but-2-yn-1-yl]oxy}quinazoline (BZ-6): IR spectra (KBr cm^{-1}): 2851 (C-H stretch), 1678 (C=C stretch), 1253 (amine, C-N stretch), 1117 (C-O stretch), 870 (Ar, C-H bend), 774 (Ar, C-H bend). ^{1}H-NMR (DMSO-d_6), δ(ppm): 1.77 (m, various protons of cyclic amine, H32, H33), 2.49 (t, various protons of cyclic amine, H30, H31), 3.44 (s, H28), 4.84 (s, H26), 7.54 (t, H23), 7.71 (d, Ar, H21), 8.18 (d, Ar, H24); ^{13}C-NMR (DMSO-d_6), δ(ppm): 46 (22), 51 (17, 21), 55 (18. 20), 56 (12), 79 (13), 80 (14), 126 (5), 127 (1, 3), 134 (2), 147 (9), 148 (6), 159 (7). Elemental analysis: for $C_{16}H_{17}N_3O$: Calcd: C, 76.49%; H, 6.77%; N, 16.73%. Found: C, 76.87%; H, 6.56%; N, 16.42%.

RESULTS AND DISCUSSION

The synthesized compounds were prepared according to scheme 2, the synthesis of 4-(prop-2-yn-1-yloxy)quinazoline (BZ) was generated through nucleophilic displacement of bromide located at 3-prop-1-yne by ionic of 4-hydroxyquinazoline. The Mannich reaction of BZ with paraformaldehyde, appropriated cyclic amine and catalytic amount of cuprous chloride, generated the desired compounds (BZ 1-6). The structures of various compounds were verified through IR, ^{1}H-NMR, ^{13}C-NMR and elemental analysis as indicated in the results. The proposed mechanism for alkylation and Mannich reaction are outlined in Schemes 3 and 4.

In order for Mannich reaction to proceed, a reactive immonium cations intermediates should be formed from condensation of paraformaldehyde and appropriate cyclic amines (Schiff base formation). The attack of the carbanion of cuprous salt of 4-(prop-2-yn-1-yloxy)quinazoline on the carbon of Schiff base generate the desired compounds (BZ 1-6).

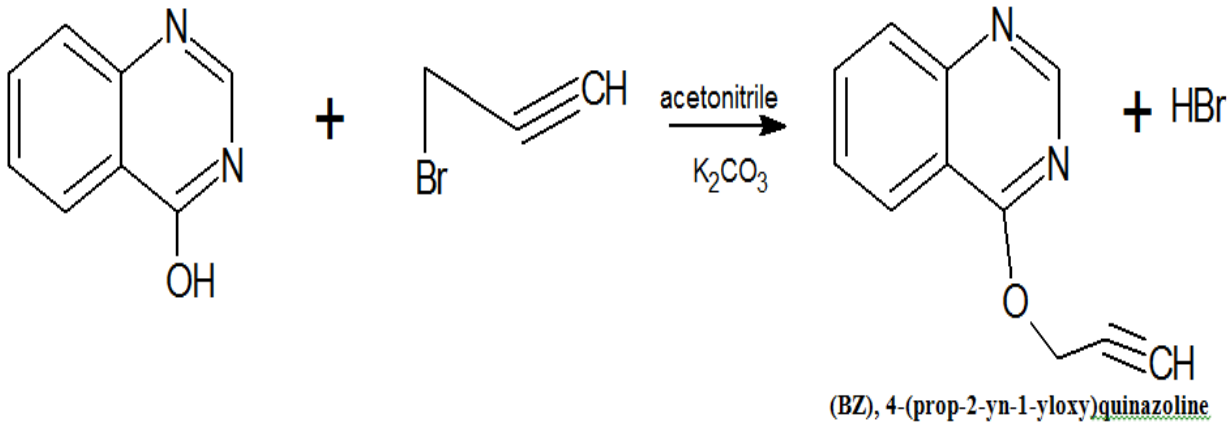

Scheme 3: Alkylation reaction of 4-hydroxyquinazoline

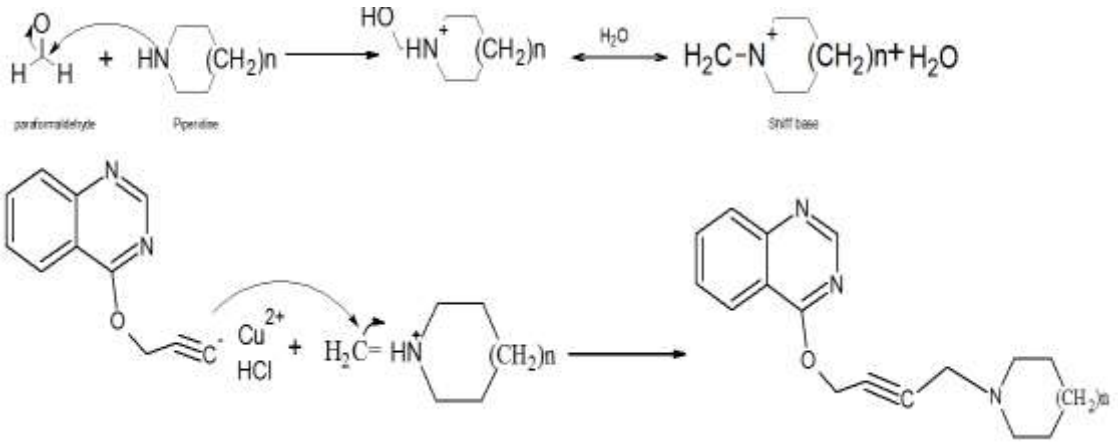

Scheme 4: Proposed Mannich reaction

Docking

Kinases inhibitors are known to have a cyclic amine that is able to make an electrostatic interaction with the backbone amide of the ATP-binding site hinge region. Also amino group could exist in the kinase inhibitor which makes a water-mediated hydrogen bond with the Thr845 hydroxyl group (also exists in the purine binding region). Additionally, they usually have a hydrophobic cyclic system that fits in a hydrophobic specificity determinant pocket on the other side of the binding site [9].

Accordingly, these compounds were designed to have a two heterocyclic system linked with each other via rigid spacer (i.e. an acetylenic group). Such a design should offer these compounds the ability to bind with the purine binding region via the first cyclic system and with the specificity binding region via the second cyclic group. The rigid linker should boost compound binding via decreasing the entropic penalty (usually associated with flexible linkers).

Docking of two compounds along with the co-crystallized ligand, lapatinib, into the ATP-binding site of the EFGR kinase domain has resulted in energetically favorable binding modes (Table 1 and Figure 5). B03 (Binding energy=-5.5 kcal/mol) has a lower binding energy than B01 (Binding energy=-5.0 kcal/mol), although it is higher than the famous EFGR-kinase inhibitor lapatinib (binding energy=-13.8 kcal/mol). Looking at the docking binding mode of B01, the quinazoline ring was perfectly aligned on the lapatinib quinazoline ring and thus was able to make the usual hydrogen bond with the hinge region backbone amide (i.e., Met793) and the usual water-mediated hydrogen bond. The other part of B03, the azepane ring, was placed on the lapatinib benzene ring at the hydrophobic specificity pocket, making van der Waals interactions with the surrounding residues. It is worth noting that the azapane protonated nitrogen seems to have no role in binding. This may have led to increase the binding energy of B03 through elevating its desolvation penalty compared to lapatinib. All in all, these compounds appear to have what it takes to be good lead compounds for the EFGR-kinase enzyme, considering their small size and the important features they have in common with lapatinib.

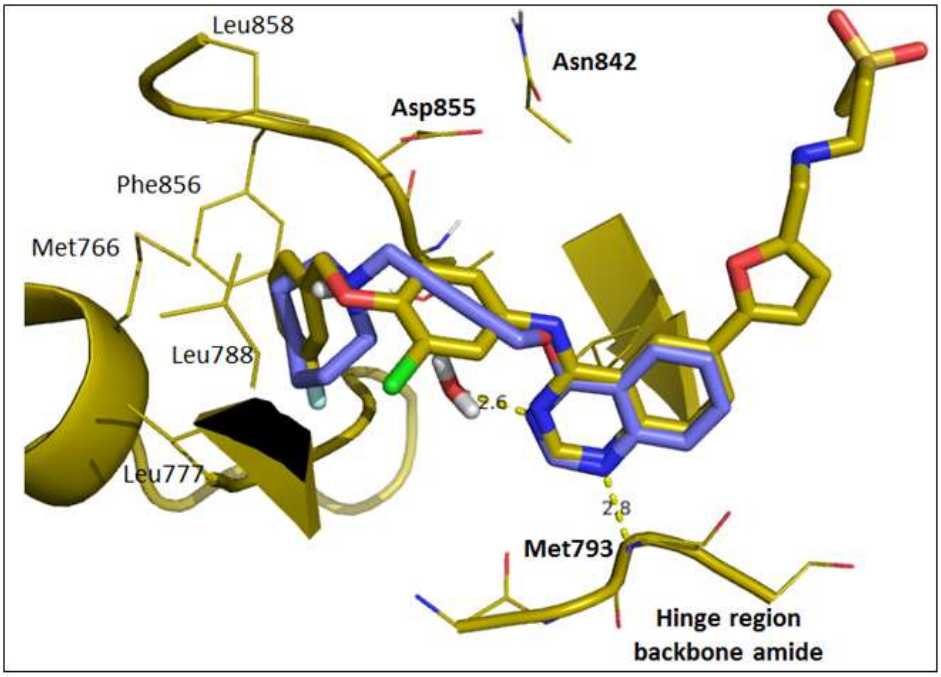

Figure 5: Shows the binding mode demonstrated by B03 (blue) in the ATP-binding site of the EGFR kinase domain (gold) along with the co-crystallized conformation of lapatinib (gold)

The picture was generated by PyMol [17]. Electrostatic interactions are shown as yellow dotted lines with distance in angstrom. Some protein chains are not shown for clarity.

Table 1: Binding energies of our docked compounds into the EFGR kinase ATP-binding site

Molecule		Autodock score (kcal/mol)
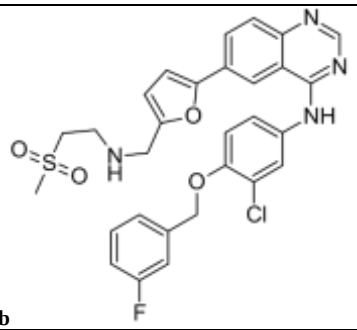 **Lapatinib**		-13.8
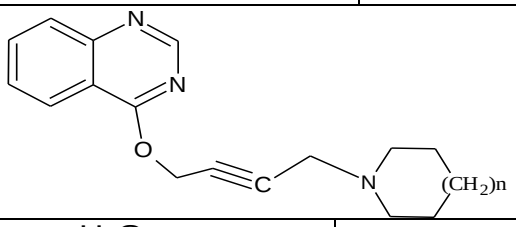		
BZ-1	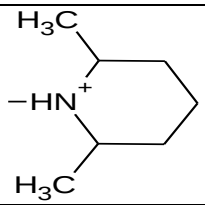	-9.5
BZ-2	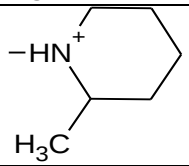	-9.2
BZ-3	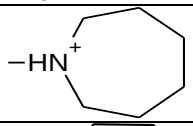	-9.6
BZ-4	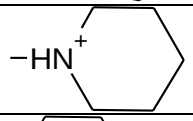	-8.8
BZ-5	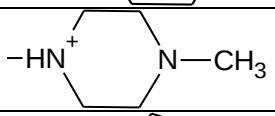	-8.0
BZ-6	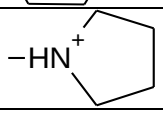	-8.0

Antiproliferative activity

The newly synthesized Aminoacetylenicoxyquinazoline derivatives were tested against breast (MCF-7) and colon cancer cell lines (Caco-2) for their antitumor activities. Interestingly, the newly synthesized compounds exhibited weak antiproliferative activities relative to the well-known standard Doxorubicin that has IC_{50} value of 2-10 uM (Table 2). Further structural modifications to enhance the antiproliferative effects will be investigated.

Table 2: The IC_{50} values (uM) of the examined compounds, values are expressed as mean ± SD of three experiments

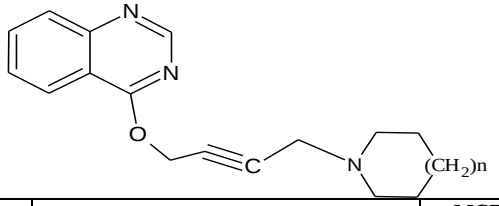			
Compound		**MCF-7**	**Caco-2**

BZ-2	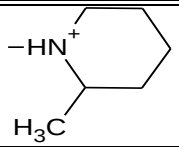	505 ± 7	468 ± 8
BZ-3	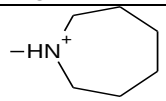	431 ± 4	379 ± 6
BZ-4	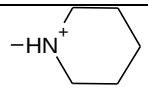	449 ± 6	352 ± 8
BZ-5	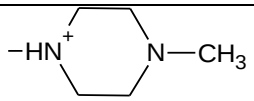	504 ± 4	492 ± 8
BZ-6	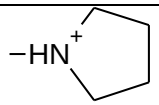	610 ± 5	644 ± 7
Doxorubicin		2-10 uM	2-10 uM

CONCLUSION

The synthesis and characterization of the new series of 4-{[4-(amino-1-yl)but-2-yn-1-yl]oxy}quinazoline (BZ 1-6) were accomplished docking of the new aminoacetylenic of 4-hydroxyquinazoline derivatives offer an effective binding with EGFR. The cytotoxicity evaluation showed promising compounds with good activities against breast and colon cancer. Further research has to be done to modify these structures to ensure greater cytotoxicity and to determine physiological and pharmacological characterization of these compounds BZ 1-6 and their new analogue.

ACKNOWLEDGMENT

The authors would like to thank the University of Petra/Faculty of Pharmacy for providing the necessary facilities to carry out this work.

REFERENCES

[1] M. Radi, E. Crespare, G. Botta, F. Falchie, G. Maga, F. Manetti, V. Corradi, M. Mancini, M.A. Santucci, S. Schenone, *Bioorg. Med. Chem. Lett*., **2008**, 18(3), 1207-1211.
[2] E. Zwich, J. Bange, A. Ullrich, *Endocrine-Related Cancer*., **2001**, 8, 161-173.
[3] E. Zwich, C. Wallsch, A. Ullrich, *Breast Disease.*, **2000**, 11, 7-18.
[4] A. Levitzki, *Pharmacol. Therap*., **1999**, 82, 231-239.
[5] A. Baker, K. Gibson, W. Grundy, A. Godfrey, J. Barlow, M. Healy, I. Richards, *Bioorg. Med. Chem. Lett*., **2001**, 11(14), 1911-1914.
[6] T.L. Edison, G.J. Patrick, *The Oncologist*., **2013**, 18(6), 653-654.
[7] A. Wakeling, S. Guy, J. Woodburn, S. Ashton, B. Curry, A. Baker, K. Gibson K, *Cancer Res*., **2002**, 62(20), 5749-5754.
[8] J. Mendelsohn, J. Baselga, *Semin. Oncol*., **2006**, 33(4), 369-385.
[9] E.R. Wood, A.T. Truesdale, O.B. McDonald, D. Yuan, A. Hassell, S.H. Dickerson, B. Ellis, C. Pennisi, E. Horne, K. Lackey, Alligood, D.W. Rusnak, T.M. Gilmer, L.A. Shewchuk, *Cancer Res*., **2004**, 64(18), 6652-6659.
[10] M.F. Sanner, *J. Mol. Graph. Mod*., **1999**, 17, 57-61.
[11] S.J. Weiner, P.A. Kollman, D.A. Case, U.C. Singh, C. Ghio, G. Alagona, S. Profeta, P. Weiner, *J. Amer. Chem. Soc*., **1984**, 106(3), 765-784.
[12] G.M. Morris, D.S. Goodsell, R.S. Halliday, R. Huey, W.E. Hart, R.K. Belew, A.J. Olson, *J. Comput. Chem*., **1998**, 19(14), 1639-1662.
[13] G.M. Morris, R. Huey, W. Lindstrom, M.F. Sanner, R.K. Belew, D.S. Goodsell, A.J. Olson, *J. Comput. Chem*., **2011**, 30(16), 2785-2791.
[14] Maestro, version 9.2, Schrödinger, LLC, New York, **2011**.
[15] W.L. Jorgensen, J. Tirado-Rives, *J. Amer. Chem. Soc*., **1988**, 110(6), 1657-1666.
[16] J. Gasteiger, M. Marsili, *Tetrahedron*., **1980**, 36(22), 3219-3228.
[17] The PyMOL Molecular Graphics System, Version 1.2r3pre, Schrödinger, LLC.